Electronic supplementary information

Simulation of Conformality of ALD Growth Inside Lateral Channels: Comparison Between a Diffusion–Reaction Model and a Ballistic Transport–Reaction Model

Jänis Järvilehto,*[a] Jorge A. Velasco,[a] Jihong Yim,[a] Christine Gonsalves,[a] and Riikka L. Puurunen*[a]

[a] Department of Chemical and Metallurgical Engineering, School of Chemical Engineering, Aalto University, P.O. Box 16100, FI-00076 AALTO, Finland.

* Corresponding authors. E-mail: janis.jarvilehto@aalto.fi, riikka.puurunen@aalto.fi

1 Model B: Impact of structure geometry on saturation profiles

Preliminary simulations were performed using the ballistic transport–reaction model to replicate the results presented in the original work by Yanguas-Gil and Elam.[1] Specifically, the goal was to obtain a similar shape at the end of the saturation profile, in a situation where the surface coverage is nearly uniform throughout the structure.

The simulation parameters were as in the base case presented in our article, except for the structure aspect ratio and the exposure durations. The simulations were performed using channel and hole geometries (*Trench* and *Via* classes in the *Machball* Python package[2]), as our article used a channel geometry and the original work by Yanguas-Gil and Elam[1] presented results generated using a hole geometry. To facilitate comparison of the results, the hole equivalent aspect ratios (EAR)[3] were identical for both structures. Two series of simulations were performed using each type of structure geometry: a series with varying exposure durations and hole equivalent aspect ratios and a series with varying exposure durations and a constant hole equivalent aspect ratio. In the former series, the hole equivalent aspect ratios were selected to be in the same order of magnitude as in the work by Yanguas-Gil and Elam:[1] 25, 50, 75, 100, 125. In the latter series, the AR of the channel was 1000, as in our article, resulting in an EAR of 500.

The exposure duration was varied in all series of simulations. For the series with varying EAR, the suitable exposure durations were estimated using the Gordon *et al.*[4] model. The hole equivalent aspect ratio, multiplied by 0.9, was inserted in the Gordon *et al.*[4] model (Ref. 4 Eq. 15) and the exposure duration was solved for. The aspect ratios and exposure durations used are shown in Table S1. For the series with constant EAR, the exposure duration was varied as in our article: 0.01, 0.1, 1, 10 and 100 s.

Table S1 Exposure durations and aspect ratios used in the ballistic transport–reaction model in the series with varying aspect ratios

t (s)	**EAR (-)**	**Channel AR (-)**	**Hole AR = EAR (-)**
0.032	25	50	25
0.12	50	100	50
0.26	75	150	75
0.46	100	200	100
0.71	125	250	125

The obtained saturation profiles are shown in Figure S1. In the series with varying channel aspect ratio (Fig. S1a), the saturation profiles show a slight, gentle decrease in surface coverage with penetration into

the channel. In the hole geometry, the saturation profiles decrease first and then plateau at the closed end of the hole, producing a similar shape as the saturation profiles presented by Yanguas-Gil and Elam (Ref. 1 Fig. 3). In the series with constant channel aspect ratio (Fig. S1b), the $t = 1$ s saturation profile shows an increase in surface coverage, a *trunk*, at the closed end of the channel. This increase in surface coverage was not observed in the hole geometry.

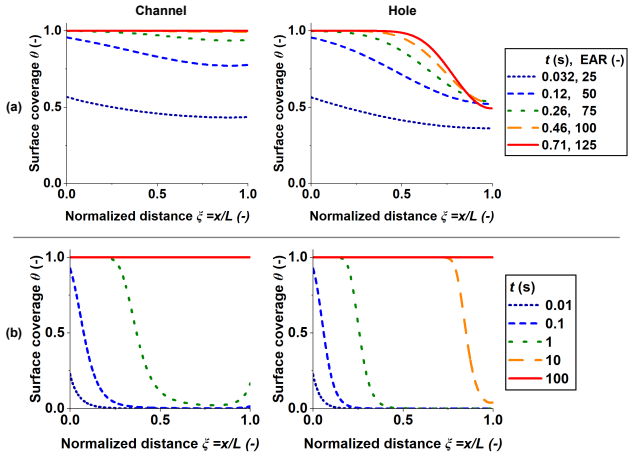

Figure S1 Series of saturation profiles generated using the ballistic transport–reaction model with two structure geometries: (left) channel and (right) hole. In panel (a), the exposure duration and hole equivalent aspect ratio were varied as indicated by the legend. The structure-specific aspect ratios are shown in Table S1. In panel (b), only the exposure duration was varied, while the EAR was constant. At 500, the aspect ratio of the channel and hole was 1000 and 500, respectively. The other simulation parameters were as in the base case presented in our article (Table 2).

2 Model B: Examination of view factors

The view factors calculated by the ballistic transport–reaction model[1] were investigated to explain the mechanism by which resolution affects the simulated saturation profiles. A channel with an aspect ratio of 1000 was discretized into 100, 1000, 2000 and 4000 segments, corresponding to resolutions of 0.1, 1, 2 and 4, respectively. The view factors between discretization segments were visualized on a two-dimensional raster, where the view factor between segments is indicated by the colour of the corresponding raster element. In addition, the impingement probability from the channel entrance and the segment areas were plotted. All of the values were calculated using the *Machball* Python package.[2]

Figure S2 shows the view factors between discretization segments, the impingement probability distri-

bution of a molecule coming from the channel entrance, as well as the areas of the discretization segments. As the resolution (*i.e.* number of discretization segments per aspect ratio unit) is increased, the view factor distribution broadens (Fig. S2, two leftmost columns). Furthermore, the impingement probability from the channel entrance decreases with increasing channel aspect ratio (Fig. S2, third column from left). The area of the channel entrance and end wall is equal to one in each case. However, the areas of the channel side wall segments vary with resolution: when the resolution is below two, the side wall segments are larger than the channel entrance and end wall (Fig. S2, rightmost column). At a resolution of two discretization segments per channel aspect ratio, all areas are equal in size (Fig. S2c, rightmost column). As the resolution is increased further, the channel side wall segments become smaller compared to the entrance and end wall segments (Fig. S2d, rightmost column). The ratio of the channel entrance area to the area of a channel side wall discretization segment S_0/S_i affects the rate of change in surface coverage $d\theta/dt$ (Eq. 14 in Ref. 1).

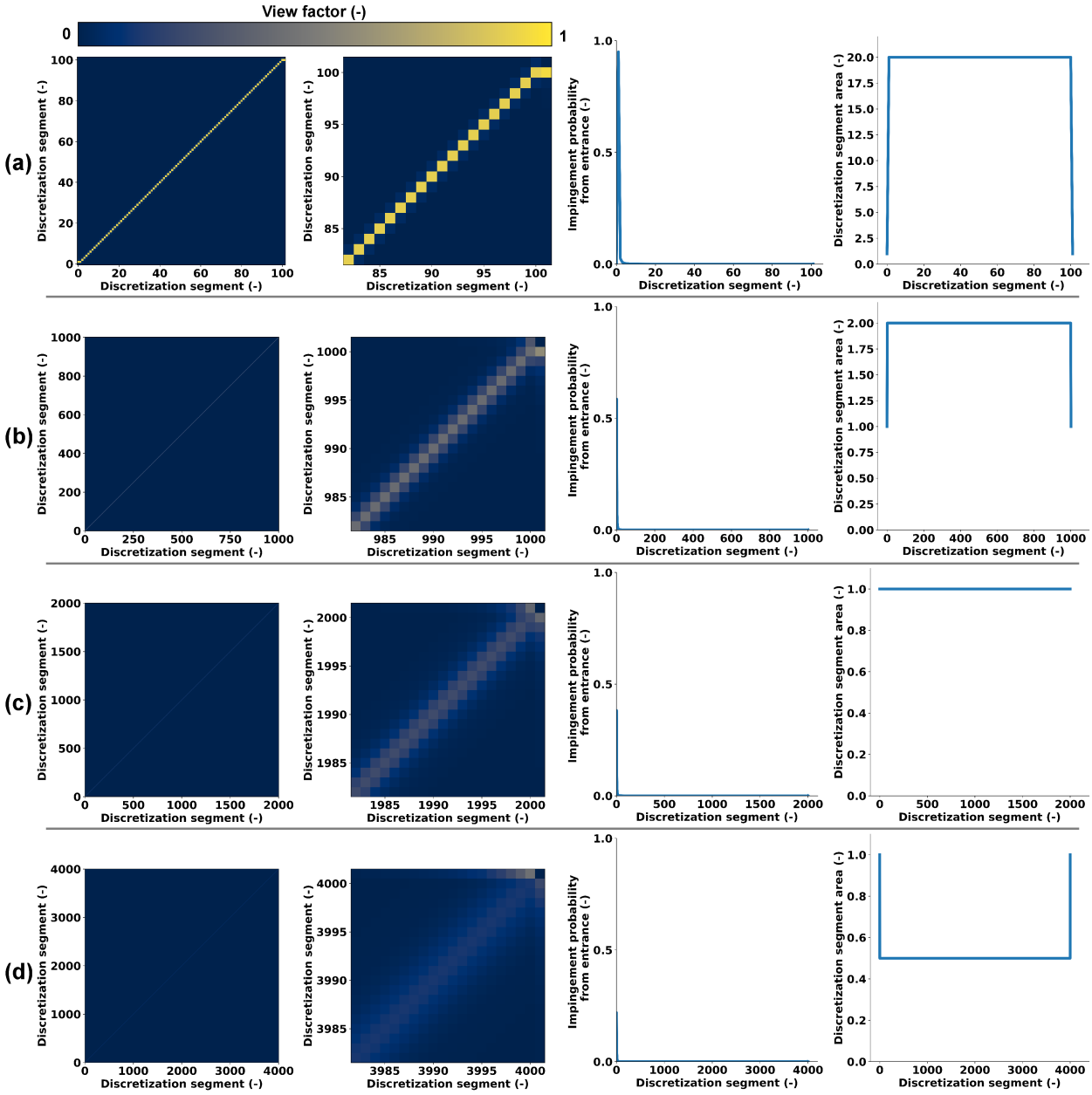

Figure S2 View factors between discretization segments, impingement probabilities from the channel entrance and segment areas for channels discretized into (a) 100, (b) 1000, (c) 2000 and (d) 4000 segments. The aspect ratio of the channel was 1000, which leads to a resolution of (a) 0.1, (b) 1, (c) 2 and (d) 4. The raster images (two leftmost columns) show the view factors between discretization segments in the whole channel and a zoomed-in view of the last 20 segments. The colour bar above the images indicates how the colours are mapped to the view factor values. The first discretization segment acts as the entrance of the channel, while the last segment marks the channel end wall. The plots (two rightmost columns) show the impingement probability from the channel entrance to each discretization segment and the area of each segment.

References

[1] A. Yanguas-Gil and J. W. Elam, *Theor. Chem. Acc.*, 2014, **133**, 1465.

[2] A. Yanguas-Gil and J. W. Elam, Machball (0.2.0), https://github.com/aldsim/machball, 2020.

[3] V. Cremers, R. L. Puurunen and J. Dendooven, *Appl. Phys. Rev.*, 2019, **6**, 021302.

[4] R. G. Gordon, D. Hausmann, E. Kim and J. Shepard, *Chem. Vap. Deposition*, 2003, **9**, 73–78.